Optical measurement of glucose content of the aqueous humor

Problem presented by

Dan Daly and Graeme Clark

Lein Applied Diagnostics

Problem statement

Many diabetics must measure their blood glucose levels regularly to maintain good health. In principle, one way of measuring the glucose concentration in the human body would be by measuring optically the glucose content of the aqueous humor in the eye. Lein Applied Diagnostics wish to assess whether this is feasible by a linear confocal scan with an LED source, or by supplementing such a system with other measurements.

Study Group contributors

Maria Aguareles (Universitat Autònoma de Barcelona)
Ksenya Arsentieva (University of Oxford)
Jon Chapman (University of Oxford)
Paul Dellar (University of Oxford)
Chris Drew (University of Nottingham)
John Fozard (University of Oxford)
David Gelder (Mathematics for Manufacturers)
Jens Gravesen (Technical University of Denmark)
Rob Hinch (University of Oxford)
Poul Hjorth (Technical University of Denmark)
Katerina Kaouri (University of Oxford)
Gregory Kozyreff (University of Oxford)
Rafael Morones (Instituto Tecnológico Autónomo de México)
John Ockendon (University of Oxford)
David Parker (University of Edinburgh)
Domingo Salazar (University of Oxford)
Morten Willatzen (University of Southern Denmark)

Report prepared by

Maria Aguareles (Universitat Autònoma de Barcelona)
John Fozard (University of Oxford)
Jens Gravesen (Technical University of Denmark)
Rob Hinch (University of Oxford)
Poul Hjorth (Technical University of Denmark)
Katerina Kaouri (University of Oxford)
David Parker (University of Edinburgh)
Morten Willatzen (University of Southern Denmark)

Problem description

Many diabetics must measure their blood glucose levels regularly to maintain good health (Appendix 1). In principle, one way of measuring the glucose concentration in the human body would be by measuring optically the glucose content of the aqueous humor in the eye. Lein Applied Diagnostics wish to assess the extent to which this is feasible

(i) purely by a system using a linear confocal scan (Appendix 2) with an LED source, as described below; and

(ii) by supplementing such a system with other suitable measurements.

The sensitivity of the refractive index of the aqueous humor to the glucose concentration is of the order of one part in 10^5 for a change in glucose concentration of 5 mg/dl, and concentrations of between 50 mg/dl and 400 mg/dl need to be detected reliably.

Confocal Scanning: the use of a confocal scanning technique enables one to measure the optical depth of the aqueous humor to this required accuracy. The optical depth, D, is given by L/n where L is the physical depth of the anterior chamber and n is the refractive index of the aqueous humor. This direct measurement cannot be made in practice as the real depth of the anterior chamber changes due to corneal swelling and accommodation of the ocular lens.

Problem 1: Is it possible to use other information obtainable from the confocal microscopy to resolve this point. In particular the measurement detects retro-reflections from the front and back of the cornea, and from the front and back of the lens, in addition to the measurements giving the location of the various surfaces. Do these retro-reflections provide the necessary information?

Problem 2: If the scan can only tell us the optical depth, what else could be measured that would enable the refractive index to be obtained to the required accuracy? In particular, can this be achieved by any of (or some combination of) the following:

(i) Taking measurements at different wavelengths of light. Two wavelengths allow the measurement of the dispersion of the aqueous humor, which is a function of the glucose concentration.

(ii) Taking several measurements, say one when the subject is focusing on infinity and one when he or she is focusing in the near-field.

(iii) Use of polarization (since glucose is optically active).

(iv) Use of spectroscopic techniques.

(v) Other suggestions.

1 Introduction

Let us start by thanking Lein Applied Diagnostics and Dan Daly and Graeme Clark for bringing a very challenging problem to the Study Group and for answering many questions during the week. We have looked into a number of different methods that potentially could provide the necessary measurement of the glucose level in the aqueous humor.

In Section 2 we investigate the original proposal by Lein to measure the optical depth at two different wavelengths. In the same section we also consider the case where one of the optical measurements is replaced by an acoustic measurement.

In the above approach the key feature is the distance between the reflected signals, but the intensity of the signals depends on the glucose concentration too. The possibility of utilizing this effect is investigated in Section 3.

One possible method to determine the refractive index, and thus the glucose concentration, of the aqueous humor would be to determine the incident ray that leads to total internal reflection. This is investigated in Section 4.

Finally, in Section 5 we investigate whether the glucose level impact on the eyesight can be used to determine the glucose concentration.

2 Length measurements

Let c be the speed of light in vacuum and consider an optical medium with length ℓ. If the speed of light in the medium is c_1 then the *refractive index* n and the *optical depth* ℓ_o are given by

$$n = \frac{c}{c_1} \qquad \text{and} \qquad \ell_o = \frac{\ell}{n}. \tag{1}$$

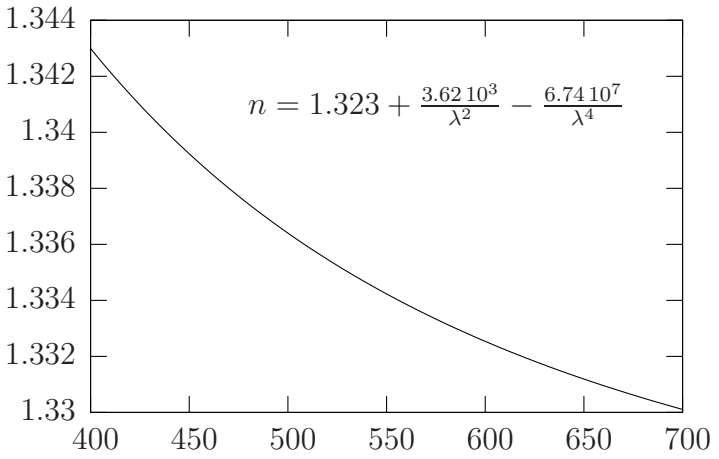

Figure 1: The refractive index of water as a function of wavelength (see [7]).

The refractive index does not depend only on the glucose concentration C but also on the free-space wavelength λ; see Figure 1. We have

$$n = a(\lambda) + C\, b(\lambda), \tag{2}$$

where $a(\lambda) = 1.323 + 3.62\,10^3\,\lambda^{-2} - 6.74\,10^7\,\lambda^{-4}$ is the refractive index of water (*cf.* Figure 1) and the value of $b(\lambda)$ was given by Lein for three different wavelengths; see Table 1.

λ	a	$b = \dfrac{\mathrm{d}n}{\mathrm{d}C}$
436 nm	1.340	$1.265\,10^{-6}$dl/mg
546 nm	1.334	$1.243\,10^{-6}$dl/mg
633 nm	1.332	$1.231\,10^{-6}$dl/mg

Table 1: The refractive index and its dependence on the glucose concentration at different wavelengths.

If we measure the optical depth at two different wavelengths then we have

$$\ell = n(\lambda_i)\ell_o(\lambda_i) = n_i\ell_i = (a_i + b_iC)\ell_i, \quad i = 1, 2. \tag{3}$$

The two linear equations in ℓ and C can easily be solved to give

$$C = \frac{\ell_1\, a_1 - \ell_2\, a_2}{\ell_2\, b_2 - \ell_1\, b_1}. \tag{4}$$

Next we want to determine the accuracy. If $\Delta\ell_i$ is the error on ℓ_i then a conservative estimate of the error on C is

$$\Delta C = \left|\frac{\partial C}{\partial \ell_1}\Delta\ell_1\right| + \left|\frac{\partial C}{\partial \ell_2}\Delta\ell_2\right|.$$

The partial derivatives are

$$\begin{aligned}
\frac{\partial C}{\partial \ell_1} &= \ell_2\,\frac{a_1\, b_2 - a_2\, b_1}{(\ell_2\, b_2 - \ell_1\, b_1)^2} = \frac{(a_1 + Cb_1)(a_2 + Cb_2)}{\ell_1(a_1b_2 - a_2b_1)} \approx \frac{a_1a_2}{\ell_1(a_1b_2 - a_2b_1)}, \\
\frac{\partial C}{\partial \ell_2} &= \frac{(a_1 + Cb_1)(a_2 + Cb_2)}{\ell_2(a_2b_1 - a_1b_2)} \approx \frac{a_1a_2}{\ell_2(a_2b_1 - a_1b_2)}.
\end{aligned}$$

So

$$\Delta C = \frac{a_1\, a_2}{|a_1\, b_2 - a_2\, b_1|}\left(\left|\frac{\Delta\ell_1}{\ell_1}\right| + \left|\frac{\Delta\ell_2}{\ell_2}\right|\right). \tag{5}$$

In the case where $\lambda_1 = 436\,\mathrm{nm}$ and $\lambda_2 = 633\,\mathrm{nm}$ we obtain

$$\frac{a_1\, a_2}{|a_1\, b_2 - a_2\, b_1|} = 5.036\, 10^7\, \mathrm{mg/dl}. \tag{6}$$

So all in all

$$\Delta C \approx 10^8 \frac{\Delta \ell}{\ell}\, \mathrm{mg/dl} \qquad \text{or} \qquad \frac{\Delta \ell}{\ell} = 10^{-8}\, \Delta C\, \mathrm{dl/mg},$$

and if we want an accuracy of 5mg/dl for the concentration then we need a relative accuracy of $5.0\, 10^{-8}$ on the length measurement. The thickness of the aqueous humor is 3 mm which the light passes twice, so we end up with a required accuracy on the length measurement of

$$5.0\, 10^{-8} \times 6\, 10^{-3}\mathrm{m} = 3\, 10^{-10}\, \mathrm{m} = 0.3\, \mathrm{nm}. \tag{7}$$

The present setup by Lein Applied Diagnostics allows the optical depths within the eye to be determined with an accuracy of 10 nm.

2.1 Acoustic measurement

Suppose we also measure the distance using ultra sound, then we can replace one of the equations (3) with

$$\ell = u\, t_a = (a_0 + b_0) t_a\,, \tag{8}$$

where u is the speed of sound in the aqueous humor. If we use linear regression on the values in Table 2, then we obtain the values

$$a_0 = 1496.81\, \mathrm{m/s}, \qquad b_0 = 3.35\, 10^{-3}\, (\mathrm{m/s})/(\mathrm{mg/dl})\,, \tag{9}$$

corresponding to the relationship shown in Figure 2.

molality	concentration	u
0.07002 mol/kg	1260.36 mg/dl	1501.02 m/s
0.10033 mol/kg	1805.94 mg/dl	1502.87 m/s
0.12004 mol/kg	2160.72 mg/dl	1504.08 m/s
0.14970 mol/kg	2694.60 mg/dl	1505.82 m/s

Table 2: The speed of sound at different glucose concentrations, see [1]. It is assumed that 1 kg is 10 dl, and that the molecular weight of glucose is 180 g.

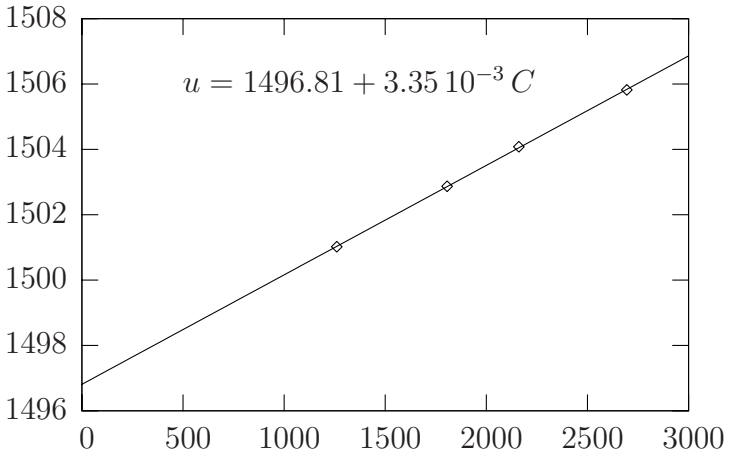

Figure 2: The speed of sound as a function of glucose concentration, see [1].

Just as before we have that the concentration is

$$C = \frac{\ell_0\, a_0 - \ell_2\, a_2}{\ell_2\, b_2 - \ell_0\, b_0}. \tag{10}$$

and that the error is

$$\Delta C \approx \left| \frac{a_0 a_2}{a_0 b_2 - a_2 b_0} \right| \left(\left| \frac{\Delta t_a}{t_a} \right| + \left| \frac{\Delta \ell_o}{\ell_o} \right| \right).$$

But now

$$\left| \frac{a_0 a_2}{a_0 b_2 - a_2 b_0} \right| = 7.7\,10^5\,\mathrm{mg/dl}\,. \tag{11}$$

We have $\ell_0 \approx 6\,\mathrm{mm}$, $\Delta\ell_0 \approx 10\,\mathrm{nm}$, and $t_a \approx 6\,\mathrm{mm}/(1500\,\mathrm{m/s}) = 4\,10^{-6}\,\mathrm{s}$, so if $\Delta t_a \approx 10^{-11}\,\mathrm{s}$ then we obtain

$$\Delta C \approx 7.5\,10^5 \left(\frac{10^{-5}}{4} + \frac{10^{-5}}{6} \right) \approx 3.125\,,$$

within the required accuracy! A search on Google on "100 GHz" seems to indicate that a time resolution at the order of $10^{-11}\,\mathrm{s}$ is within reach; see [9].

3 Intensity measurements

Consider a multi-layered slab with layer index i. Figure 3 shows the case of two finite layers and two semi-infinite layers. Electromagnetic waves are assumed to propagate

along the x direction with the electric field component polarized along the y direction. It follows that all electric field components in the various layers are polarized in the y direction as well. The interface to the right of slab i corresponds to the location x_i along the x axis (normal incidence conditions). From Maxwell's equations it follows that monochromatic electromagnetic waves satisfy (with time dependence $\exp(-i\omega t)$ [8])

$$i\omega\mu\vec{H} = \vec{\nabla} \times \vec{E}. \tag{12}$$

and continuity applies everywhere to the tangential components of the $\vec{E}$ and $\vec{H}$ fields. Hence, omitting the time factor $\exp(-i\omega t)$ in all terms,

$$E_i^{>} \exp(ik_i x_i) + E_i^{<} \exp(-ik_i x_i) = E_{i+1}^{>} \exp(ik_{i+1} x_i) + E_{i+1}^{<} \exp(-ik_{i+1} x_i),$$

$$-\frac{n_i}{\mu_i u_0} \left(E_i^{>} \exp(ik_i x_i) - E_i^{<} \exp(-ik_i x_i)\right) = -\frac{n_{i+1}}{\mu_{i+1} u_0} \left(E_{i+1}^{>} \exp(ik_{i+1} x_i) - E_{i+1}^{<} \exp(-ik_{i+1} x_i)\right), \tag{13}$$

where $i = 1, 2, \ldots, N$, u_0 is the speed of light in vacuum, μ_i is the permeability of layer i, n_i is the refractive index of layer i, and N denotes the number of interfaces in the slab. The superscript $>$ ($<$) indicates propagation along (against) the x-axis direction (see also Figure 3).

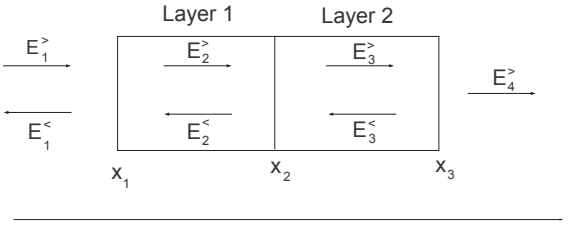

Figure 3: Schematic view of the slab structure and propagating waves.

We assume that the incoming electromagnetic wave $E_1^{>}$ is a known quantity impinging on the interface x_1 from a semi-infinite medium extending to $x = -\infty$. We also assume that the medium located to the right of the last interface is semi-infinite (extending to $x = \infty$), *i.e.* $E_{N+1}^{<} \equiv 0$ since we ignore scattering mechanisms in the semi-infinite media. The above system of equations is a set of $2N + 2$ linear equations in the $2N + 2$ unknowns $E_1^{<}, E_2^{>}, E_2^{<}, ..., E_N^{>}, E_N^{<}, E_{N+1}^{>}$, which can be solved so as to get the amplitude of the reflected wave $E_1^{<}$. Having determined $E_1^{<}$, we can compute the intensity I_R of the reflected wave as compared to the incoming intensity

$$I_R = \frac{|E_1^{<}|^2}{|E_1^{>}|^2}. \tag{14}$$

Note that the wavenumber k_i depends on the refractive index n_i of layer i according to the relation

$$k_i = \frac{\omega n_i}{u_0}. \tag{15}$$

Hence, the intensity is sensitive to the glucose concentration since the refractive index of the aqueous humor layer (here, for simplicity, assumed to be layer N) depends on the glucose concentration.

If we only consider the reflection from the front of the aqueous humor, then we have a slab with width d, representing the cornea. At one side of the slab there is air, while at the other side there is the aqueous humor. So n_1 is the refractive index of the air, n_2 the refractive index in the cornea and n_3 the refractive index in the aqueous humor. The concentration C is related to n_3 through

$$n_3 = n_{30} + \frac{\mathrm{d}n_3}{\mathrm{d}C} C \tag{16}$$

where n_{30} is a reference refractive index (in an aqueous humor without glucose). The squared reflection coefficient is a function of n_3, n_1, n_2, d, and ω (the frequency of the incident light), given by

$$|I_R|^2 = \frac{(\frac{n_1-n_2}{n_1+n_2})^2 + (\frac{n_2-n_3}{n_2+n_3})^2 + 2(\frac{n_1-n_2}{n_1+n_2})(\frac{n_2-n_3}{n_2+n_3})\cos(\frac{2\omega n_2}{c_0}d)}{1 + (\frac{n_1-n_2}{n_1+n_2})^2(\frac{n_2-n_3}{n_2+n_3})^2 + 2(\frac{n_1-n_2}{n_1+n_2})(\frac{n_2-n_3}{n_2+n_3})\cos(\frac{2\omega n_2}{c_0}d)}. \tag{17}$$

Using (17) we plot in Figure 4 $|I_R|^2$ as a function of the refractive index n_3. We take the following values: $n_1 = 1$, $n_2 = 1.336$, and $n_{30} = 1.332$ corresponding to the wavelength $\lambda = 633$nm as read off from the last row of Table 1. From the same row we read off the value $\frac{\mathrm{d}n_3}{\mathrm{d}C} = 1.231 \times 10^{-6}$. We note that the changes in n_3 with C are of the order of 10^{-6} for all three wavelengths in Table 1. The other parameters used are the speed of light $u_0 = 3 \times 10^8$m/s and the slab width $d = 0.5$mm, taken as a representative width of the cornea (even though there are bound to be large fluctuations to this value).

Since $n_1 \leq n_3 \leq n_2$, we choose the values for $n_1 = 1$ and $n_2 = 1.336$ as the minimum and maximum values for the plotting range in in Figure 4. We see that $|I_R|^2$ decreases monotonically with n_3.

Then we use the relation (16) in (17) to plot in Figure 5 $|I_R|^2$ as a function of C. In Figure 6 we plot $\frac{\mathrm{d}|I_R|^2}{\mathrm{d}C}$ as a function of C. We find that this derivative is of the order of 10^{-7}. Since the measurements by Lein have a 10^{-5} accuracy, the sensitivity of $|I_R|^2$ with n_3 is not sufficient for our purposes. We also are interested in plotting n_3 as a function of $|I_R|^2$. We thus let $X = (n_1 - n_2)/(n_1 + n_2)$ and $Y = (n_2 - n_3)/(n_2 + n_3)$ and $\alpha = \cos(\frac{2\omega n_2}{c_0}d)$ and solve (17) for n_3/n_2, to obtain

$$\frac{n_3}{n_2} = \frac{-1 + |I_R|^2 + M}{-1 + |I_R|^2 - M}, \tag{18}$$

where

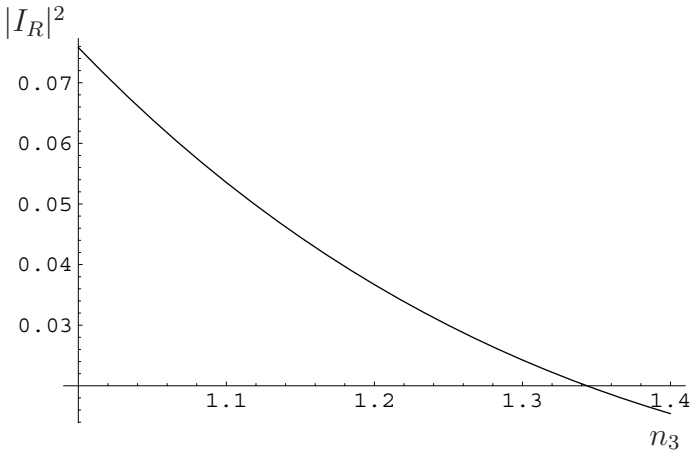

Figure 4: $|I_R|^2$ versus n_3.

$$M = \sqrt{|I_R|^2 + (-1 - |I_R|^4 + (-1 + |I_R|^2)\alpha^2))X^2 + |I_R|^8} - \alpha X + |I_R|^2 \alpha X. \qquad (19)$$

Then we use (18) to plot, in Figure 7, n_3 as a function of $|I_R|^2$. The two horizontal lines on the figure represent the values of $n_1 = 1$ and $n_2 = 1.336$ within which n_3 should be restricted. In Figure 8 we plot $\dfrac{dn_3}{d|I_R|^2}$ versus $|I_R|^2$. The horizontal axis runs from $|I_R|^2_{\min} = X^2 = 0.0206887$ to $|I_R|^2_{\max} = 0.0770474$, corresponding respectively to $n_3 = n_1$ and $n_3 = n_2$.

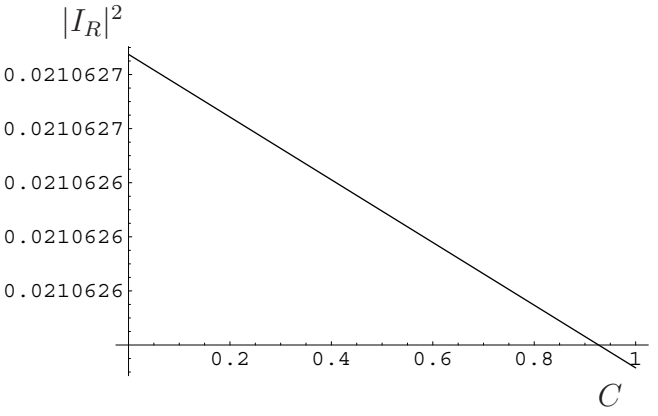

Figure 5: $|I_R|^2$ versus C.

3.1 Incorporation of absorption in material layers

Finally, we note that material absorption exists in each layer. This can easily be accounted for by modifying the expression for the wavenumber in layer i according to

$$k_i \rightarrow k_i + i\alpha_i \qquad (20)$$

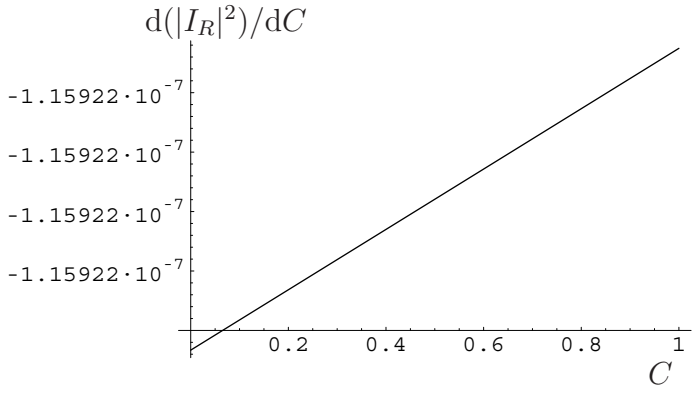

Figure 6: $\frac{\mathrm{d}|I_R|^2}{\mathrm{d}C}$ versus C.

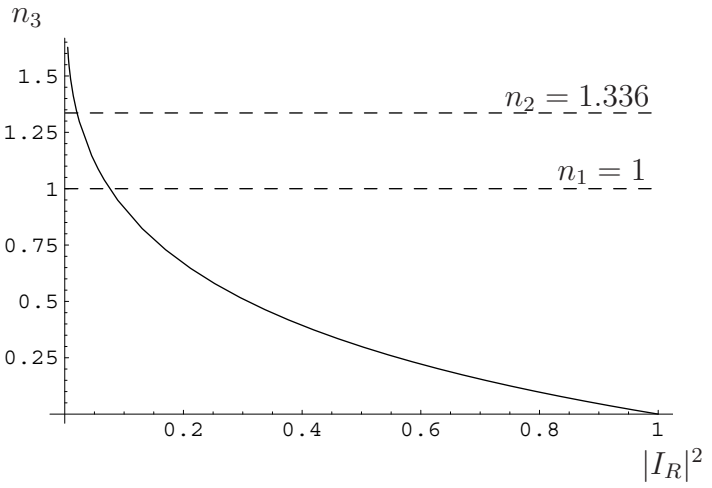

Figure 7: n_3 versus $|I_R|^2$.

for forward-propagating waves, and

$$k_i \to k_i - i\alpha_i \tag{21}$$

for backward-propagating waves. Here, α_i is the absorption coefficient in layer i, which is expected to be highly dependent on the light wavelength and a function of the glucose concentration for layer N where glucose is present. We have

$$\alpha_N = \alpha_N^0 + \frac{d\alpha}{dC}C, \tag{22}$$

where α_N^0 and C are the absorption coefficient in layer N in the absence of glucose and the glucose concentration, respectively. Thus, information about $\frac{d\alpha}{dC}$ allows the glucose concentration to be estimated by measuring the intensity drop as a function of glucose concentration (a convenient choice of light wavelength is a light wavelength where the

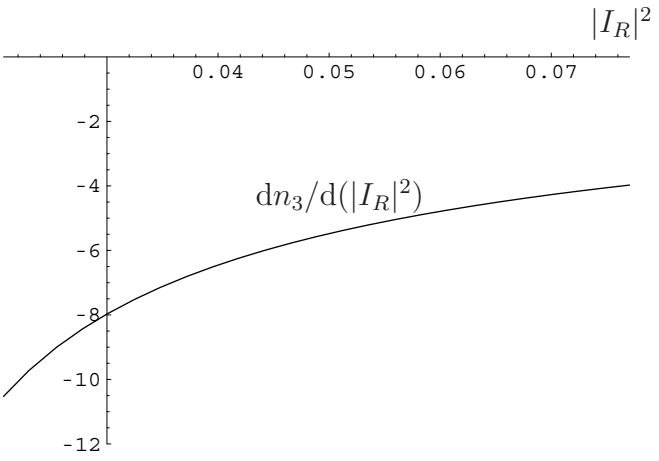

Figure 8: $\dfrac{dn_3}{d|I_R|^2}$ versus $|I_R|^2$.

absorption of glucose is as high as possible). Especially, a combination of time-pulsed signals and such intensity measurements are likely to provide the best estimate of the glucose concentration since both the layer thicknesses (*i.e.* the locations x_i) as well as the glucose concentration can be estimated independently.

4 Is Total Internal Reflection (TIR) possible?

One possible method to determine the refractive index of the aqueous humor n_3 would be to determine (by trial and error) the incident ray that leads to TIR.

4.1 Flat interfaces

We assume that ray theory approximation is sufficient for the purpose of determining whether or not TIR is possible. Therefore applying Snell's law at the air-cornea and cornea-aqueous humor interfaces (see Figure 9) we get respectively

$$n_1 \sin\theta_1 = n_2 \sin\theta_2, \quad n_2 \sin\theta_2 = n_3 \sin\theta_3$$

and this gives

$$\sin\theta_1 = \frac{n_3}{n_1} \sin\theta_3$$

For internal reflection we set $\sin\theta_3 = 1$ and this implies that $\sin\theta_1 = n_3/n_1$ which is impossible because we always have $n_3 > n_1$ (some typical values are $n_1 = 1$ and $n_3 = 1.33$). Therefore TIR is not achievable at any angle of incidence.

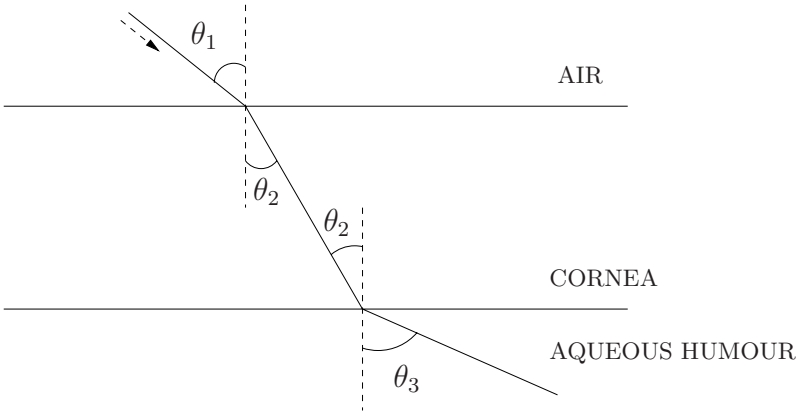

Figure 9: Schematic of the geometry assuming the air-cornea and cornea-aqueous humor interfaces are flat; θ_1 is the angle made with the normal and the incident ray.

4.2 Curved interfaces

We now investigate whether taking into account the fact that the two interfaces are actually curved may compensate for the difference between n_1 and n_3 that does not permit TIR for flat interfaces. We take the two interfaces to be arcs of concentric circles. The outer radius is OA and inner radius is OB. In Figure 10 (left) we show a ray incident

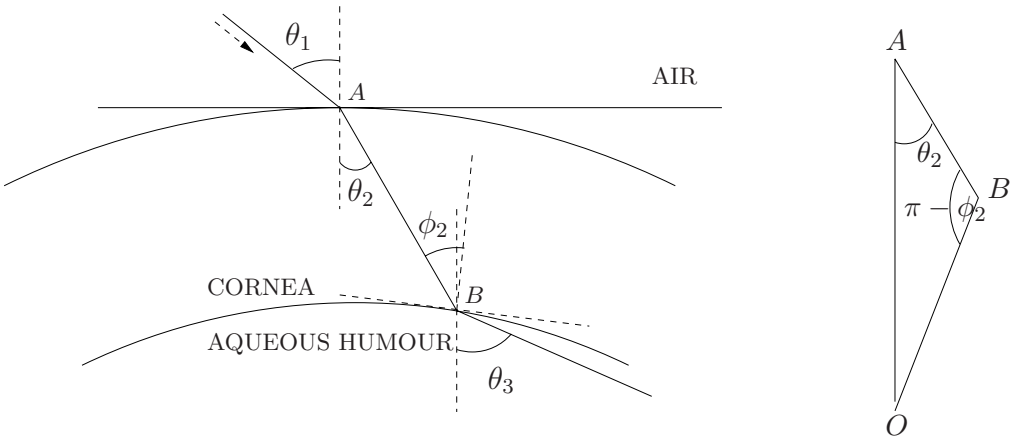

Figure 10: Schematic of the geometry assuming the air-cornea and cornea-aqueous humor interfaces are flat: θ_1 is the angle made with the normal and the incident ray

at angle θ_1 to the normal. It refracts at the first interface and the refraction angle is θ_2. (Up to this point the problem is the same as in Section 4.1.) However when the ray hits the second interface the angle made with the normal is $\phi_2 = \theta_2 + \beta$ where β is precisely the angle increment due to the curvature of this second interface (on purpose we show

this as a very small angle on Figure 10). From the sine rule for the triangle OAB (see Figure 10, right picture) we have

$$\frac{OA}{\sin\phi_2} = \frac{OB}{\sin\theta_2}\,. \tag{23}$$

Writing Snell's law again for the two interfaces we have

$$n_1 \sin\theta_1 = n_2 \sin\theta_2, \quad n_2 \sin\phi_2 = n_3 \sin\phi_3. \tag{24}$$

From (23) and (24) we have

$$\sin\theta_1 = \frac{(OB)n_3}{(OA)n_1} \sin\theta_3. \tag{25}$$

Therefore for TIR to be possible when accounting for curvature we need

$$\frac{(OB)n_3}{(OA)n_1} \leq 1. \tag{26}$$

However, since $OB \sim 7.30$ mm, $OA \sim 7.80$ mm, $n_1 = 1$ and $n_3 = 1.33$, condition (26) cannot be satisfied. Therefore we conclude that TIR is not possible even when we account for curvature of the interfaces.

5 Shape of the lens

5.1 Clinical Observations

The effects of blood glucose concentration on the refractive properties of the eye have been a conundrum for some time [13]. Large changes in blood glucose concentration, such as those found in undiagnosed diabetics and those in the early stages of controlling their blood glucose, can have a dramatic effect on eyesight [16].

A number of clinical surveys, typically examining patients at the onset of treatment ([14], [10] among others), have found an initial hyperopic (more long-sighted) change in the eye as fasting blood glucose concentrations decreased. The patients' eyesight then gradually returned to normal over a period of several months. However, in one study the opposite change was observed, with the patients becoming more hyperopic as their blood glucose concentrations increased [4].

Although this is an important effect, a controlled diabetic needs to monitor smaller changes in blood sugar levels over a time-scale of minutes, not weeks. There are only a few clinical studies of such acute optical changes. In Steffes [15], a change in blood glucose concentration of approximately 50 mg/dl yielded a change in refractive correction of approximately 0.3 dioptres (D or m^{-1}) over a time period of about of 60 minutes, with little time-lag between the two changes. Here a reduction in blood glucose produced a reduction in the refractive correction of the eye, which was measured with an auto-refractometer. It should be noted that this appears to be the results of just one experiment repeated once.

Gwinup and Villareal [5] found in 6 patients that acute changes in blood glucose concentration of approximately 150mg/dl yielded changes in refractive correction of about 0.75 D, where the subject became more myopic/less hyperopic as the glucose concentration increased. The opposite change occurred in 4 aphakic patients (those whose eyes have no lens), suggesting that the myopic change is due to changes in the properties of the lens.

5.2 Power calculation for refractive index of eye

We now perform a simple power calculation to test the hypothesis that these changes in the refractive correction are due purely to changes in the refractive index of the aqueous humor.

Model of eye

The actual geometry of the eye is moderately complicated, with a layered structure for the crystalline lens. The Bennett-Rabbets model (Figure 11) is a standard simple model of the eye, which approximates the lens as a material of uniform refractive index, and the cornea as an interface between the aqueous humor and air (effectively ignoring its thickness). These approximations are likely to have little effect on the order of magnitude of the calculations of the power. It is possible to calculate the power of the eye without making these approximations by numerically solving the eikonal equation of geometrical optics with a variable refractive index. However, for our order of magnitude estimate this is not necessary.

The length scales involved in the eye are all much greater than the wavelength of light, and therefore we use geometrical optics considering only paraxial rays (those which make a small angle with the principal axis of the system). This approximation is called Gaussian optics (see for example Ramsey [12] or Born and Wolf [2]), and gives a simple approximation of the total power of the eye P (see later calculation). The power P is defined as $\frac{n_v}{f}$, where f is the focal length of the eye. We assume that the refractive correction is equal to the strength of external lens required to correct the patient's vision, and that the geometry of the eye is constant in each experiment. (This ignores the effect of varying accommodation between the experiments, but it seems likely that this is dealt with in the refractometry measurements.) Hence the focal length f will be constant once

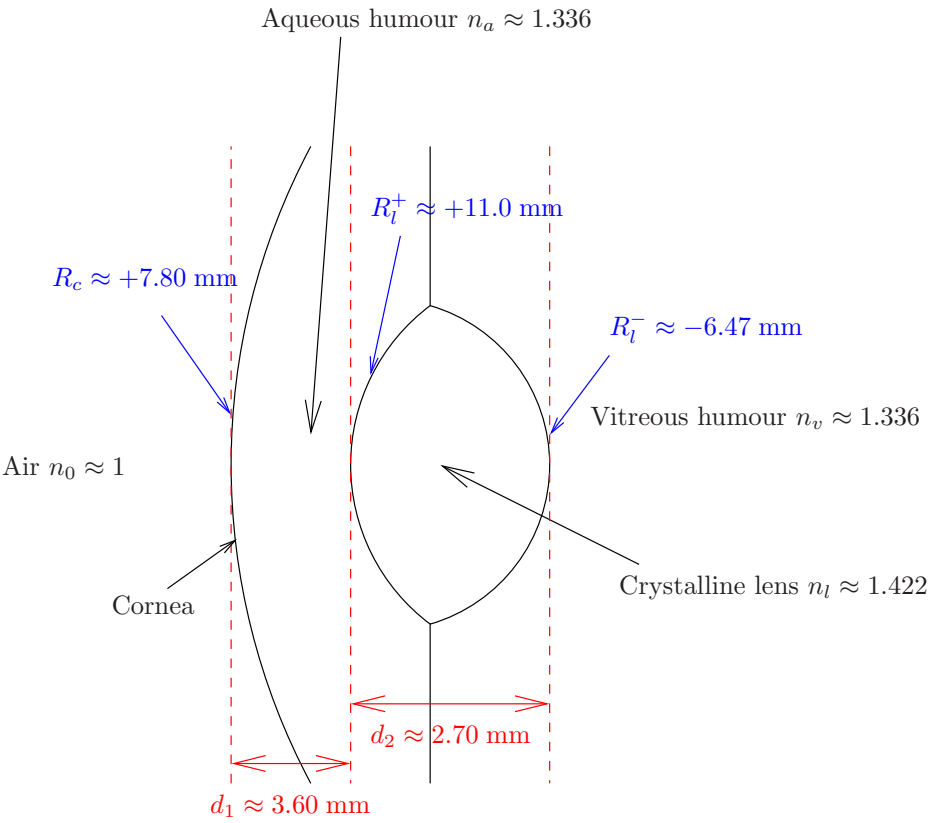

Figure 11: Simple model of eye, after Rabbets [11].

the patient's eyesight has been corrected for. The linear changes in P (from its definition as $\frac{n_v}{f}$) are of the order of 10^{-5} and can be ignored; therefore the total power of the eye and the correcting lens must be approximately constant. The distance between the eye and the correcting lens can be ignored since it is small compared with the focal length of such correction (and is also constant), so the total power is simply the sum of the power of the eye and the power of the correcting lens. Hence changes in the measured quantity are equal to minus those changes in the power of the eye P.

Ignoring the distances between the refracting surfaces of the eye, we find that

$$P \approx \frac{n_a - n_0}{R_c} + (n_l - n_a)\frac{1}{R_l^+} + (n_a - n_l)\frac{1}{R_l^-}, \tag{27}$$

or using the values for the radii of curvature of the surfaces from Figure 11,

$$P \approx (-128n_0 - 119n_a + 247n_l)\ \mathrm{D}. \tag{28}$$

A 5mg/dl change in the glucose concentration of the aqueous humor changes n_a by approximately 10^{-5}, so this effect can only explain a change in P of the order 10^{-2} D. This is significantly less than the change in refractive correction detected in clinical studies, which strongly suggests that there is another mechanism at play. Moreover, the changes observed in the clinical studies are within the practical tolerance of the measurement device.

More detailed power calculation

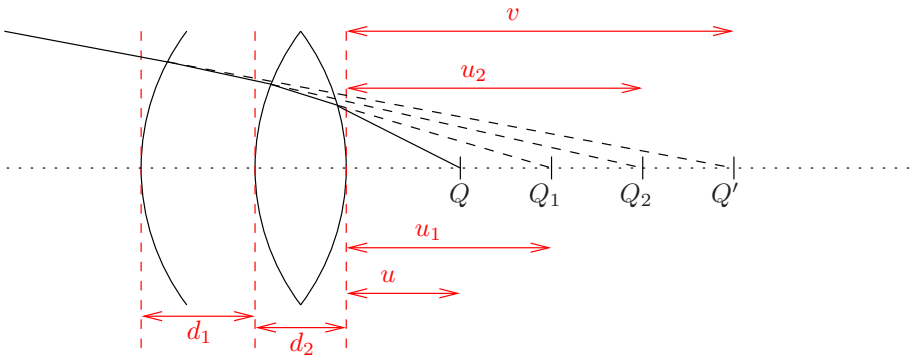

Figure 12: Ray paths for calculation of total power of eye.

Figure 12 show a pencil of rays incident from the left converging on the point Q'. Let Q_2 be the focus of the rays after refraction at the cornea, Q_1 be the focus after refraction at the front surface of the lens, and Q be the focus after refraction at the rear surface of the lens. Applying the standard result for paraxial refraction (see Ramsey [12] Chapter IV Art. 60) at each interface yields

$$\frac{n_0}{v+d_1+d_2} - \frac{n_a}{u_2+d_1+d_2} = \frac{n_0-n_a}{R_c} \tag{29}$$

$$\frac{n_a}{u_2+d_2} - \frac{n_l}{u_1+d_2} = \frac{n_a-n_l}{R_l^+} \tag{30}$$

$$\frac{n_l}{u_1} - \frac{n_v}{u} = \frac{n_l-n_v}{R_l^-}\,. \tag{31}$$

In the case of the eye, u, u_1, u_2 and v are all greater than the distance from the rear of the lens to the retina ($\approx 16\times10^{-3}$m), so to a first approximation we may neglect the terms d_1 and d_2 in the denominators of (29)–(31). These equations then simplify to the earlier approximation of the power of the eye (27). The errors in making these approximations are of the order of $\frac{d_1+d_2}{u^2} \approx 0.03\,\mathrm{D}$, so our earlier approximation (27) is valid.

5.3 Alternative explanations for clinical changes

In the clinical studies previously mentioned, the mechanism by which these changes occur is somewhat contentious. However, it seems to be the case that these are due to changes in the properties of the lens - such as thickening, changes in hydration due to osmotic effects, or changes in refractive index. The biochemistry involved is poorly understood and rather complex due to a number of competing effects (see the editorial by Roxburgh [13]).

5.4 Possible method of measuring glucose concentration

Despite the controversy over the underlying mechanism, there is a correlation between the properties of the eye and blood glucose concentration, which is measurable for the changes in blood glucose levels experienced by diabetic patients. Moreover, using the simple model we see that the relative changes are of the order of 10^{-4} for a 5mg/dl change in blood glucose levels. This yields a changes in optical path length of 10^{-7} m, which is measurable using the confocal microscope.

In the simplified model, the refractive properties of the lens depend upon three factors: the front and rear curvatures of the lens, and its refractive index. For a particular patient, one would expect that these three properties would in turn depend only upon two variables: the degree of accommodation of the eye (how much the ciliary muscles are contracting) and the glucose concentration. The device developed by Lein can make three measurements of the lens: the distance between reflections from the front and back surfaces of the lens, which gives the of the optical depth of the lens; and the two retro-reflections which give the radii of curvature of the two surfaces (although these measurements will be indirect because the light must pass through the cornea, aqueous humor and for the rear reflection the lens itself, and at each interface the pencil of rays will be refracted). Therefore we have two unknown parameters and three measurements, so in principle we can determine the glucose concentration. In practice the functional dependence of glucose concentration on these measurements will vary greatly from person to person and would have to be determined experimentally. Further measurements can be obtained by making the patient vary the level of accommodation of the lens by varying the focal point. Note that for each focal point, we can make three new measurements of the lens but only introduce one new unknown (the level of accommodation).

The physiology of the eye is much more complicated than the simple models discussed in this report. For example, the relationship between lens properties and glucose concentrations is likely to be history-dependent (both with a time lag of a few minutes, and long term changes), the lens has a more complicated structure than that assumed here, and there are likely to be other factors such as blood pressure which also affect the optical properties of the eye. It is possible that one of these complications could dominate the changes in power due to the instantaneous glucose concentration. Currently, there is insufficient experimental data of the short-term effect of changes in glucose levels on the optical properties of the eye.

6 Conclusion

We have investigated a number of potential methods to measure the glucose concentration in the aqueous humor. In summary, our findings are:

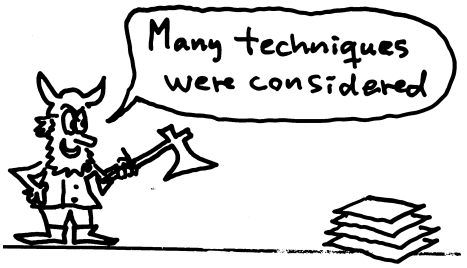

(i) Measuring optical depth at two different wavelengths: Does not work.

(ii) Measuring optical and acoustic depth: Might work, depending on the ability to time acoustic pulses with an accuracy of 10^{-11}s.

(iii) Measuring intensity: Does not work.

(iv) Measuring total internal reflection: Does not work.

(v) Measuring the shape of the lens: Needs further investigation.

Little worked.

Our calculations are done under idealized assumptions, *e.g.* we have used values for glucose in pure water, but we believe that the order of magnitudes we find are are correct.

Besides the approaches reported here a few others were considered during the week of the Study Group. One was using a lens with multiple focal lengths, but it did not lead to any useful results. Another was to measure the absorption spectrum, but nothing was quantified.

As a final remark we note that if the time for one measurement is sufficiently short, then it is possible to make several measurements of the glucose level in a short time. If we take the average of say one hundred measurements, then the expected error will be one tenth of the error on the individual measurements.

References

[1] Asbjørn Aarflot. *Partial Molar Properties of Aqueous Monosaccharide Solutions at Elevated Pressure*, Cand. Scient. Thesis, Physical Chemistry, University of Bergen, March 2001, Bergen, Norway.
http://www.ub.uib.no/elpub/2001/h/415001/Hovedoppgave.pdf

[2] N. Born and E. Wolf. *Principles of Optics*. Pergamon, 2nd edition, 1964.

[3] Barbera Dobler and Rolf Bendl. Precise modelling of the eye for proton therapy of intra-ocular tumours, *Phys. Med. Biol.* **47**:593–613, 2001.
http://stacks.iop.org/PMB/47/593

[4] P.R. Eva, P.T. Pascoe, and D.G. Vaughan. Refractive changes in hyperglycaemia: hyperopia, not myopia. *British Journal Of Opthalmology*, **66**:500–505, 1992.

[5] G. Gwinup and A. Villareal. Relationship of serum glucose concentration to changes in refraction. *Diabetes*, **25**(1):29–31, 1975.

[6] Jeffrey J. Heys, Victor H. Barocas, and Michael J. Taravella. Modeling passive mechanical interaction between aqueous humor and iris, *J. Biomechanical Eng.* **123**:540–547, 2001.
http://www.iovs.org/cgi/content/full/43/3/700

[7] Indiana University Physics Department. *P309: Intermediate Physics Laboratory #28: Refraction and Dispersion*
http://physics.indiana.edu/~p309f01/28_refracdisp.pdf

[8] L.D. Landau, E.M. Lifshitz, and L.P. Pitaevskii. *Electrodynamics of Continuous Media*. Course of Theoretical Physics Vol. 8, Second Edition, Butterworth Heinemann Ltd., 1984.

[9] Otto L. Muskens. *High-Amplitude, Ultrashort Solitons in Solids*, Thesis, Universiteit Utrecht, Holland, 2004.
http://www.phys.uu.nl/~muskens/thesis.pdf

[10] F. Okamoto, H. Sone, T. Nonoyama, and S. Hommura. Refractive changes in diabetic patients during intensive glycaemic control. *British Journal of Opthalmology*, **84**:1097–1102, 2000.

[11] R. B. Rabbets. *Bennet and Rabbets' Clinical Visual Optics*. 1998.

[12] A. S. Ramsey. *Elementary Geometrical Optics*. G. Bell and Sons, 1914.

[13] S. Roxburgh. The conundrum of sweet hyperopia. *British Journal of Opthalmology*, **84**:1088–1089, 2000.

[14] Y. Saito, G. Ohmi, S. Kinoshita, Y. Nakamura, K. Ogawa, M. Harino, and S. Okada. Transient hyeropia with lens swelling at initial therapy in diabetes. *British Journal of Opthalmology*, **77**:145–148, 1993.

[15] P. G. Steffes. Laser-based measurement of glucose in the occular aqueous humor: An efficacious portal for determination of serum glucose levels. *Diabetes Technology and Theraputics*, **1**(2):129–133, 1992.

[16] M. J. Willi. Hyperopia and hyperglycemia (letter). *Survey of Opthalmology*, **41**(2):187, 1996.

[17] Kamal Youcef-Toumi and Vidi A. Saptari. *Noninvasive Blood Glucose Analysis using Near Infrared Absorption Spectroscopy*, MIT Home Automation and HealthCare consortium, Progress Report 2-5, 2000. `http://darbelofflab.mit.edu/ProgressReports/HomeAutomation/Report2-5/Chapter04.pdf`

Appendix 1

Diabetes is a large and growing problem. The International Diabetes Federation estimates that some 194 million people worldwide have diabetes today. In the UK, 3.9% of the adult population in the UK is diabetic. By 2025, the number of diabetics is forecast to jump to 333 million worldwide. In this market, glucose self-monitoring is essential for identifying when a diabetic's blood sugar level is too low, in which case they may have seizures, or too high, which can lead to blindness and invalidity in the longer term.

The current 'finger stick' method of measuring blood glucose is a multi-step process that is particularly difficult for young and elderly patients, or those with impaired vision or motor control. The user pierces her skin with a lancet to draw blood, applies the blood to a test strip, and then inserts the strip into a meter from which the glucose value is read. This process is painful, risks infection, can damage nerves and is unpopular, especially with young children and teenagers.

Appendix 2

The confocal technique works as shown in Figure 13. The principle of the process is that

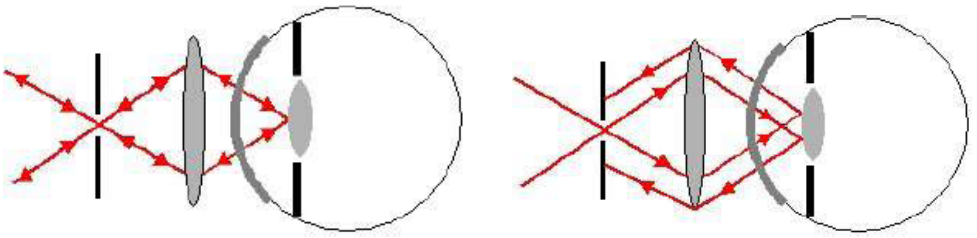

(a) Eye in focus (b) Eye out of focus

Figure 13: Principle of confocal measurement.

if the surface of one of the components of the eye is at the focal point of the measurement lens (as in Figure 13(a)) light will be retro-reflected along its original path and will pass through the small pinhole. This light will then fall on a detector and a large intensity signal is seen. If no surface is at the focal point (as in Figure 13(b)) the reflected light diverges and hardly any makes it back through the pinhole. The detector therefore registers a low intensity signal.

This technique can be applied to the measurement of the refractive index as described below. An outline concept of a test system is shown in Figure 14.

As the scanning lens is moved backwards and forwards a bright image will be seen on the detector when the returning light reflected from the eye is focussed through the pinhole stop. At each interface (cornea/aqueous humor, aqueous humor/lens *etc.*) there will be light reflected such that during the scan the intensity profile shown in Figure 15 will be generated.

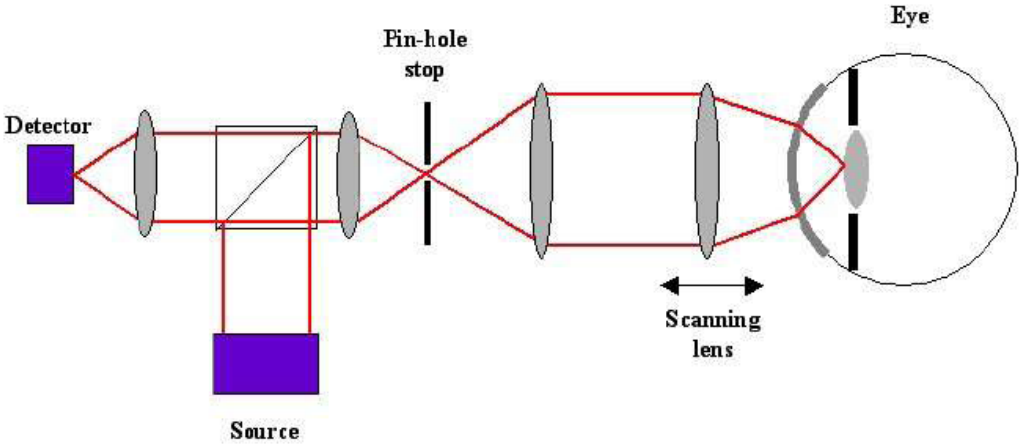

Figure 14: Confocal arrangement to measure the refractive index of the aqueous humor.

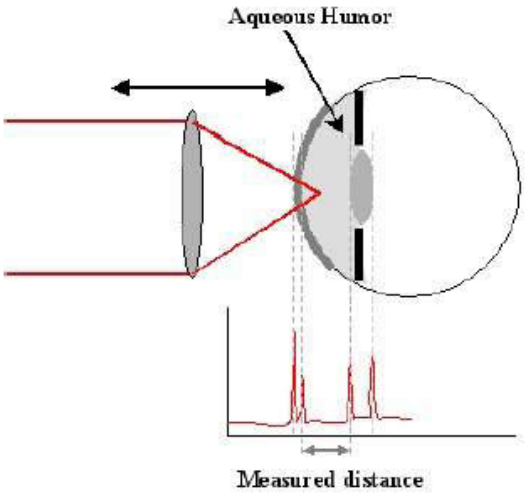

Figure 15: Intensity profile seen during the scan

The physical distance moved by the scanning lens between the two central intensity peaks is directly related to the refractive index of the aqueous humor. The glucose concentration can therefore be calculated by knowing the position of the scanning lens when a bright image is seen on the detector.